

## Copolymerizing Behavior and Processability of Benzoxazine/Epoxy Systems and Their Applications for Glass Fiber Composite Laminates

Mingzhen Xu, Xulin Yang, Rui Zhao, Xiaobo Liu

Research Branch of Functional Materials, Institute of Microelectronic and Solid State Electronic, High-Temperature Resistant Polymers and Composites Key Laboratory of Sichuan Province, University of Electronic Science and Technology of China, Chengdu 610054, People's Republic of China

Correspondence to: X. B. Liu (E-mail: liuxb@uestc.edu.cn)

**ABSTRACT:** Copolymerizing behavior and processability of epoxy/benzoxazine containing cyano groups (EP/BA-ph) systems were investigated by differential scanning calorimetry and dynamic rheological analysis. The results showed that EP/BA-ph systems exhibited two characteristic peaks corresponding to ring-opening of benzoxazine and ring-formation of cyano groups, respectively. Compared with BA-ph, EP/BA-ph copolymer processability was improved and can be controlled by varying EP contents, processing temperature, and time. Then EP/BA-ph copolymers were employed to prepare EP/BA-ph/glass fiber (GF) composite laminates and their mechanical, morphological, and thermal properties were investigated. Compared with those of BA-ph/GF composites, the flexural strength, and modulus of EP/BA-ph/GF composites with 50 wt % EP content were increased by 13.5 and 20%, respectively. The enhancements in mechanical properties are mainly due to the strong interfacial adhesions between GF and matrices, which was confirmed by SEM observations. All EP/BA-ph/GF composite laminates are stable up to 510°C in air. EP/BA-ph/GF laminates will have potential applications in the areas where require of excellent mechanical properties and high temperature resistance. © 2012 Wiley Periodicals, Inc. *J. Appl. Polym. Sci.* 000: 000–000, 2012

**KEYWORDS:** copolymers; mechanical properties; thermal properties

Received 5 June 2012; accepted 27 July 2012; published online

**DOI:** 10.1002/app.38422

### INTRODUCTION

Glass fiber (GF)/polymer composite laminates are well known for their high strength and modulus, excellent stiffness and creep resistance, low density, and dimensional stability. Those laminates have been considered as next-generation high-performance materials for aircraft and ground facility applications<sup>1</sup> and the most promising materials in numerous fields such as aerospace,<sup>2</sup> automotive,<sup>3</sup> wind energy harvesting,<sup>4,5</sup> and deep-sea exploration.<sup>6</sup> The performance of the GF/polymer composites could vary a lot depending on the types of GFs, matrices, and fiber–matrix interface.<sup>7,8</sup> It was soon realized that the main obstacle in the use of GF/polymer composite laminates was weak interfacial interactions between GFs and polymer matrices which results in inefficient load transfer and phase separation. Thus, molecular level design of the GF-polymer laminate interface is essential for the fabrication of high-performance composite materials.

Recently, the benzoxazine-based phenolic resins have attracted significant attention. Compared with the conventional phenolic resins, benzoxazine-based phenolic resin possesses outstanding

advantages: nearly zero shrinkage, low water absorption, high glass transition temperature, high char yield, very long shelf life, no requirement of curing agents, no release of by-products and thus crack-free structures.<sup>9–13</sup> However, the chain transfer during the ring-opening polymerization of benzoxazine usually led to the reduce of molecular weight, low cross linking degree and low decomposition temperature, which is detrimental to mechanical and thermal properties of benzoxazine-based composites. In addition, benzoxazine-based phenolic resin usually exhibits relatively high initial viscosity, which is disadvantageous to its processability such as mixing with other components or removing air bubbles.<sup>14</sup> In our previous work,<sup>15,16</sup> cyano groups have been successfully introduced into benzoxazine monomer to polymerize<sup>17–20</sup> for improving the thermal stabilities of benzoxazine and the final cured products can stand high temperature up to 364°C. However, its processability needs to be further improved.

Epoxy (EP) resins are well-known for their outstanding properties such as mechanical properties, good chemical resistances and excellent processability. EP resins-based composites have

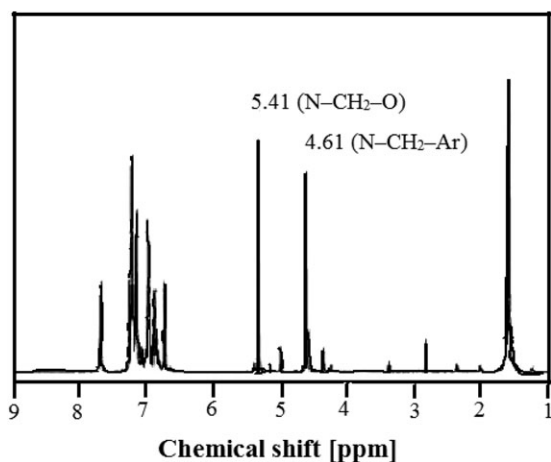


Figure 1.  $^1\text{H}$  NMR spectrum of the BA-ph in  $\text{CDCl}_3$ .

been extensively used in various fields such as aerospace,<sup>21</sup> coatings,<sup>22</sup> adhesives,<sup>23</sup> and electrical insulating materials.<sup>24</sup> However, their disadvantages are the poor thermal and thermal-oxidative stabilities.

In this study, to expand various advantages and applications of benzoxazine and EP materials, especially in the fields required high mechanical and thermal properties, we are expecting to improve the processability of benzoxazine and the interface of final GF-filled benzoxazine laminates through copolymerizing benzoxazine with epoxy with the help of the low viscosity, excellent wetting properties, and bond forming of epoxy. Thus, bisphenol A (BA)-based benzoxazine containing cyano groups (BA-ph) was synthesized and the BA-based EP was chosen to promote the compatibility between benzoxazine and EP. The copolymerizing behavior and processability of BA-ph/EP systems were investigated by differential scanning calorimetric and dynamic rheological analysis. Furthermore, the mechanical, morphological, and thermal properties of GF-filled benzoxazine/epoxy composite laminates were investigated. The results showed that GF-filled benzoxazine/epoxy composites exhibited much better mechanical and interfacial properties than GF-filled benzoxazine composites and all EP/BA-ph/GF composites could stand high temperatures up to 470°C.

## EXPERIMENTAL

### Materials

Bisphenol-A, paraformaldehyde, 1,4-dioxane, 3-aminophenol, anhydrous potassium carbonate ( $\text{K}_2\text{CO}_3$ ), and toluene were obtained from Tianjin BODI chemicals. The 4-nitrophthalonitrile was obtained from Alpha Chemical (Dezhou). Dimethyl sulfoxide (DMSO) was purchased from Tianjin Guangfu Fine Chemical Research Institute. The 3-aminophenoxyphthalonitrile (3-APN,  $T_m = 174^\circ\text{C}$ ) was synthesized from 4-nitrophthalonitrile and 3-aminophenol according to Ref. 16. Epoxy resin (diglycidyl ether of bisphenol A (DGEBA)) with epoxide equivalent weight of 213–244 was kindly supplied by Blue Star New Chemical Material. All the reagents were of analytical grade and used without further purification.

### Synthesis of Benzoxazine Containing Cyano Units (BA-ph)

The synthetic route of BA-ph monomer was synthesized according to the Ref. 16 reported before with minor modifications. In a typical experiment, 3-APN (47.00 g, 0.20 mol), bisphenol A (22.80 g, 0.10 mol), paraformaldehyde (12.00 g, 0.40 mol), and 1,4-dioxane (60 mL) and toluene (10 mL) were mixed under a stirrer at a speed of 300 rpm. After being refluxed at  $100^\circ\text{C}$  for 5 h, the reaction mixture was cooled to room temperature and slowly poured into distilled water in the formation of a solid. The solid was filtered and washed five times with distilled water. Then the yellow solid was dried in a vacuum at  $60^\circ\text{C}$  overnight. The molecular structure of BA-ph was verified by  $^1\text{H}$  NMR (Figure 1) and FTIR (Figure 2) spectroscopy.  $^1\text{H}$  NMR (300 MHz,  $\text{CDCl}_3$ )  $\delta$  (ppm): 1.40–1.52 ( $\text{CH}_3$ ), 4.61 ( $\text{N}-\text{CH}_2-\text{Ar}$ ), 5.41 ( $\text{N}-\text{CH}_2-\text{O}$ ), 6.25–6.28 ( $\text{N}-\text{Ar}-\text{H}$ ), 6.62–6.64 (ortho to  $\text{N}-\text{Ar}$ ).<sup>18</sup> The protons attached to the oxazine ring were observed at 4.61 and 5.41 ppm (Figure 1). FTIR (KBr,  $\text{cm}^{-1}$ ): 2231  $\text{cm}^{-1}$  ( $-\text{CN}$ ), 956  $\text{cm}^{-1}$  (trisubstituted benzene ring attached with oxazine ring), 1171 and 832  $\text{cm}^{-1}$  (stretch  $\text{C}-\text{N}-\text{C}$ ), 1248, 1002  $\text{cm}^{-1}$  (stretch,  $\text{C}-\text{O}-\text{C}$ ), 1419  $\text{cm}^{-1}$  ( $\text{CH}_2$  bending vibration).<sup>15,18</sup> Meanwhile, the absorption band at 2232, 1171, 832, 1248, and 1002  $\text{cm}^{-1}$  were assigned to the stretching vibration of cyano groups ( $-\text{CN}$ ),  $\text{C}-\text{N}-\text{C}$  of oxazine and  $\text{C}-\text{O}-\text{C}$  of oxazine. These  $^1\text{H}$  NMR and FTIR data were found to be in good agreement with the proposed structures.

### Preparation of EP/BA-ph Copolymers

The EP/BA-ph thermosetting copolymers with different ratios (EP content: 30, 40, and 50 wt %) were prepared by melt blending at  $100^\circ\text{C}$  for 10 min. As a reference, the pure BA-ph was prepared similarly.

### Preparation of EP/BA-ph/GF Composite Laminates

The preparation of the EP/BA-ph/GF composite laminates was carried out as follows. Various amounts of EP/BA-ph copolymers obtained above were dissolved into acetone to get a viscous solution. Then, GF cloth ( $20 \times 20 \text{ cm}^2$ ) was brush-coated

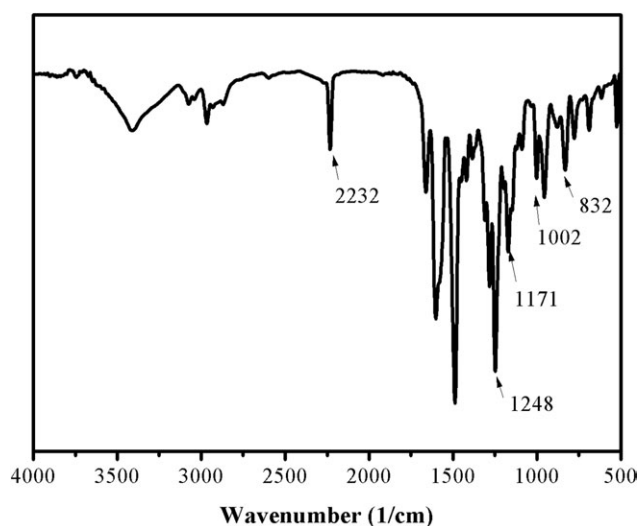
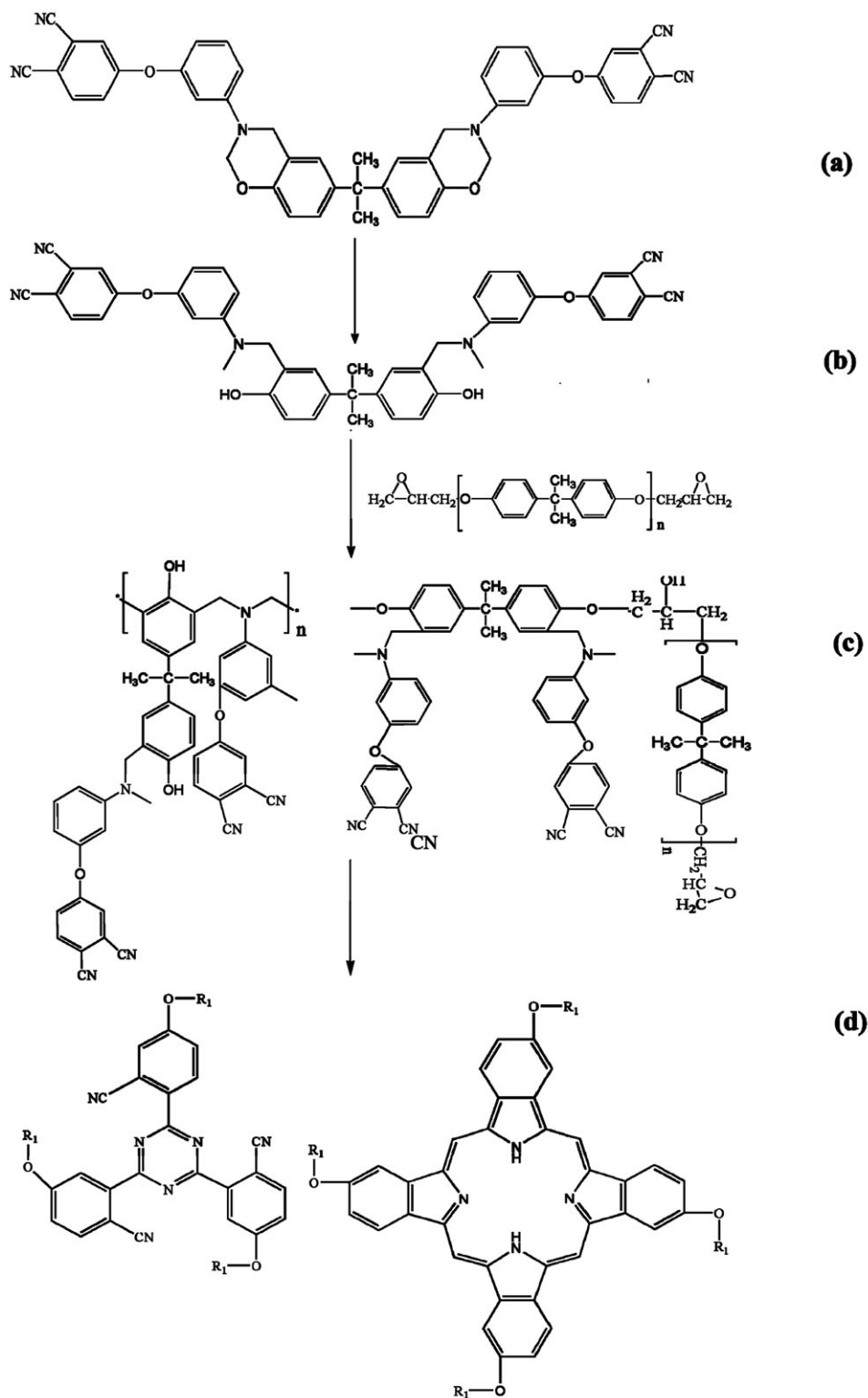


Figure 2. FTIR spectra of BA-ph monomer.



**Figure 3.** The chemical structures of (a) BA-ph monomer; (b) ring-opening of BA-ph monomer; (c) possible copolymerization of BA-ph/EP blends; and (d) final copolymerization products.

with the viscous solution obtained above and dried at room temperature for 24 h. The ratio was designed to give a prepreg of 40% copolymers and 60% GF by weight. Twenty layers of GF

prepreg cloth was placed in a stainless steel mold and hot-pressed under a pressure of 20 MPa at 200°C for 2 h, 230°C for 3 h, 260°C for 3 h, and 280°C for 3 h, respectively.

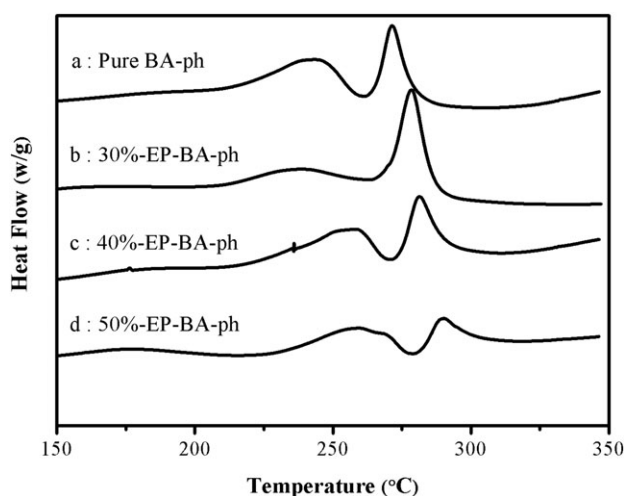


**Figure 4.** DSC curves of (a) pure BA-ph; (b) 30 wt % EP/BA-ph; (c) 40 wt % EP/BA-ph; and (d) 50 wt % EP/BA-ph.

### Characterizations

Differential scanning calorimetric (DSC) analysis was performed by TA Instruments Modulated DSC-Q100 at a heating rate of  $10^{\circ}\text{C min}^{-1}$  and a nitrogen flow rate of  $50\text{ mLmin}^{-1}$ . FTIR spectra were recorded with Shimadzu FTIR8400S Fourier Transform Infrared spectrometer in KBr pellets between  $4000$  and  $400\text{ cm}^{-1}$  in air. Dynamic rheological analysis was performed using TA Instruments Rheometer AR-G2 with a frequency of  $1\text{ Hz}$  at different temperatures in air. The samples ( $0.5\text{--}1\text{ g}$ ) were melted between  $25\text{ mm}$  diameter parallel plates with an environmental testing chamber of the rheometer. The flexural tests of the composite laminates were performed with a SANS CMT6104 series desktop electromechanical universal testing machine at room temperature. Flexural tests (three-point bending mode) were held according to the GB/T9341-2008 standard test method with a crosshead displacement speed of  $10\text{ mmmin}^{-1}$  and the test fixture was mounted in a  $10\text{ kN}$  capacity. The samples (dimension:  $80\text{ mm} \times 15\text{ mm} \times 2\text{ mm}$ ) were tested with a support span/sample thickness ratio of  $15:1$ , and gained as average value for every three samples. The morphology of the fractured surfaces of the composites were observed by SEM (JSM2 5900LV) operating at  $20\text{ kV}$ . Thermal gravimetric analysis (TGA) was performed on a TA Instruments TGA Q50 with a heating rate of  $20^{\circ}\text{C min}^{-1}$  (under nitrogen or air) and a purge of  $40\text{ mLmin}^{-1}$ .

## RESULTS AND DISCUSSION

### Copolymerizing Behavior of EP/BA-ph Systems

The possible copolymerizing processes of EP/BA-ph systems were given in Figure 3 and DSC was first employed to investigate the effect of different EP contents on the copolymerizing behavior of the EP/BA-ph systems, as shown in Figure 4. Pure BA-ph exhibited two characteristic exothermic peaks: the broad peak at  $225^{\circ}\text{C}$  corresponds to the ring-opening of the BA-ph and the copolymerization between EP and BA-ph, as shown in Figure 3(b, c); the sharp exothermic peak at  $265^{\circ}\text{C}$  was assigned to the triazine ring formation from the cyclotrimerization of cyano groups in phthalonitrile,<sup>25,26</sup> as depicted in Figure 3(d).

With the incorporation and increase of EP resin contents, those two exothermic peaks were observed to shift to higher temperatures. This is because that the EP in the system of EP/BA-ph acted as a diluent, which would retard the polymerization of BA-ph. The curing reaction would occur preferentially at around  $220^{\circ}\text{C}$  and the oxazine ring-opening polymerization produced Mannich bridge ( $-\text{CH}_2-\text{NR}-\text{CH}_2-$ ) with phenolic hydroxyl functional groups [Figure 3(b, c)]. The polymerization among BA-ph monomers was predominant in the temperature range from  $210$  to  $240^{\circ}\text{C}$ . Then the free phenolic hydroxyls with active hydrogen generated from the ring-opening reaction of BA-ph at elevated temperatures may promote the further ring-opening reaction of BA-ph and epoxy resins, and EP/BA-ph copolymers containing active phenolic hydroxyls were finally formed. As the temperature increases to about  $270^{\circ}\text{C}$ , the polymerization of cyano groups was catalyzed by the active phenolic hydroxyls produced from the ring-opening of BA-ph and the phthalocyanine and triazine were finally formed [Figure 3(d)].<sup>20,27-31</sup>

The copolymerizing behaviors of EP/BA-ph systems were also confirmed by the time sweep curves of the rheological tests, shown in Figure 5. As can be seen, in the EP/BA-ph system ( $40\text{ wt \% EP}$ ), the storage modulus ( $G'$ ) increased sharply from  $3\text{ min}$  to  $10\text{ min}$ , it was observed that copolymers had been transferred from viscosity flow state to solid state. At the same time, the loss modulus ( $G''$ ) also increased. Based on the principle of classical rheological theory, the gelation time (determined from the crossover point of  $G'$  and  $G''$ ) was observed at  $3$  and  $8\text{ min}$ , which corresponded to the ring-opening of benzoxazine rings and ring-formation of cyano groups, respectively.<sup>14</sup> The  $\tan \delta$  curve exhibited two peaks at  $4$  and  $7\text{ min}$ , which meant that the  $40\text{ wt \% EP/BA-ph}$  copolymer could polymerize well under certain curing temperature ( $255$  and  $285^{\circ}\text{C}$ ), which were consistent with the DSC observations.

### Processability of EP/BA-ph Copolymers

The complex viscosity ( $\eta^*$ ) of EP/BA-ph copolymers as a function of temperature from  $150$  to  $250^{\circ}\text{C}$  were shown in Figure 6. Before  $180^{\circ}\text{C}$ , the  $\eta^*$  of all EP/BA-ph copolymers was low. Around  $180^{\circ}\text{C}$ , there is a slight increase of  $\eta^*$ , however, a rapid increase of  $\eta^*$  is observed at  $200^{\circ}\text{C}$  for all EP/BA-ph

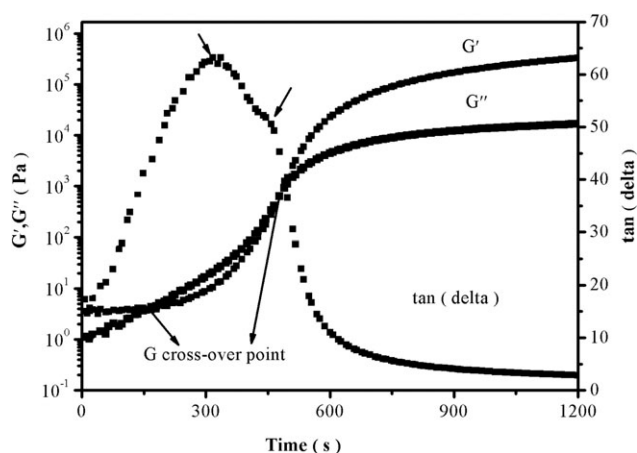


**Figure 5.** Storage modulus ( $G'$ ) and loss modulus ( $G''$ ) curves of EP/BA-ph copolymers with  $40\%$  EP content at  $200^{\circ}\text{C}$ .



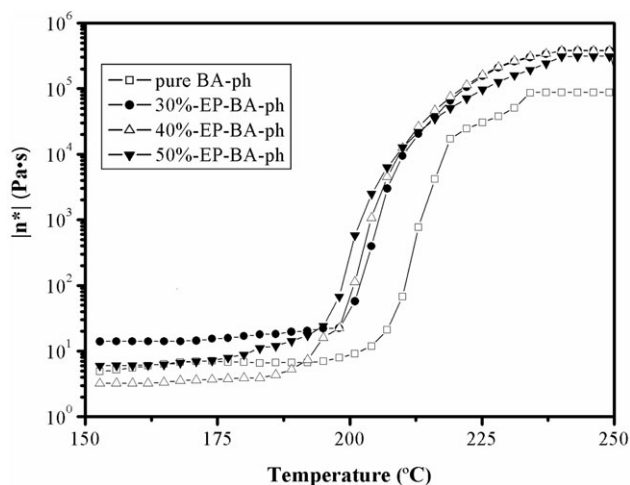


**Figure 6.** Complex viscosity curve as a function of temperature for EP/BA-ph copolymers.

copolymers. At 200°C, the  $\eta^*$  of EP/BA-ph copolymers increases with the increase of EP, indicating that the rate of polymerization is increased regularly. These results indicated that the polymerization of BA-ph was progressing at the ranges from 180 to 200°C, in well agreement with DSC results in Figure 3.

To further determine the processing temperature and time for EP/BA-ph copolymers, the  $\eta^*$  change of the EP/BA-ph copolymer with 40 wt % EP concentration was measured as a function of time at several temperatures, shown in Figure 7. It can be seen that the  $\eta^*$  at different temperatures were relatively low and stable before the final curing reaction occurred. However, after the curing reaction started, the  $\eta^*$  increased dramatically. Nevertheless, the time for dramatic  $\eta^*$  increase was varied with the different temperatures. Namely, the  $\eta^*$  increase of EP/BA-ph copolymer at 180°C took a very long time (1300 s), indicating that the reaction was carried out slowly. Quite the opposite, the  $\eta^*$  increase of EP/BA-ph copolymers at 220°C took a rather short time, revealing that curing reaction was carried out very fast. Thus, 200°C is a proper processing temperature for

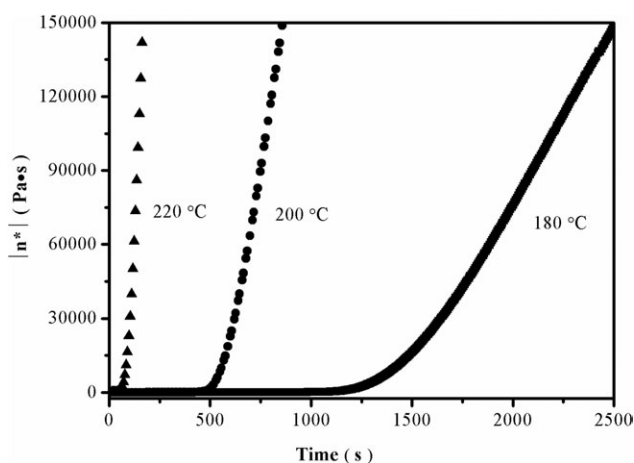


**Figure 7.** Complex viscosity as a function of time for the 40% EP/BA-ph copolymer at various temperatures.

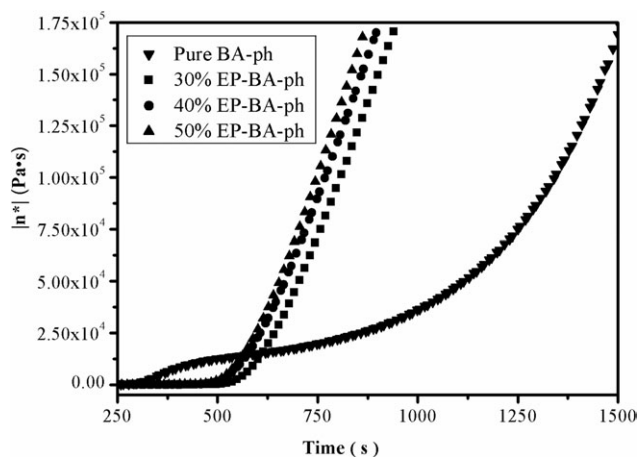


**Figure 8.** Complex viscosity as a function of time at 200°C for EP/BA-ph copolymers.

EP/BA-ph copolymers. On the one hand, these results manifested that the  $\eta^*$  of the EP/BA-ph copolymer processed faster with the increase of processing temperature. On the other hand,

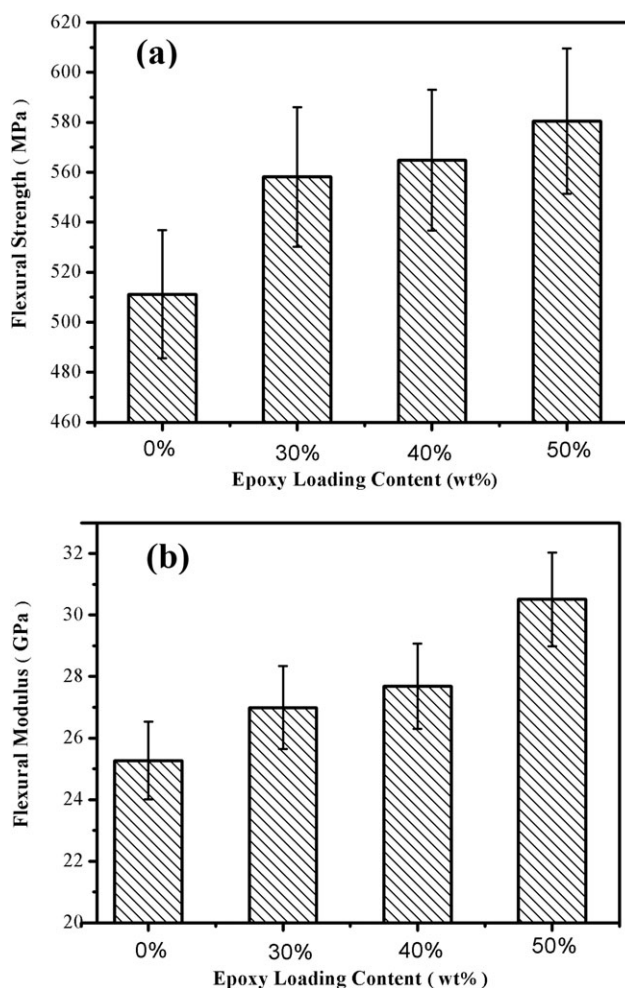


**Figure 9.** Mechanical properties of EP/BA-ph/GF composite laminates: (a) flexural strength, (b) flexural modulus.

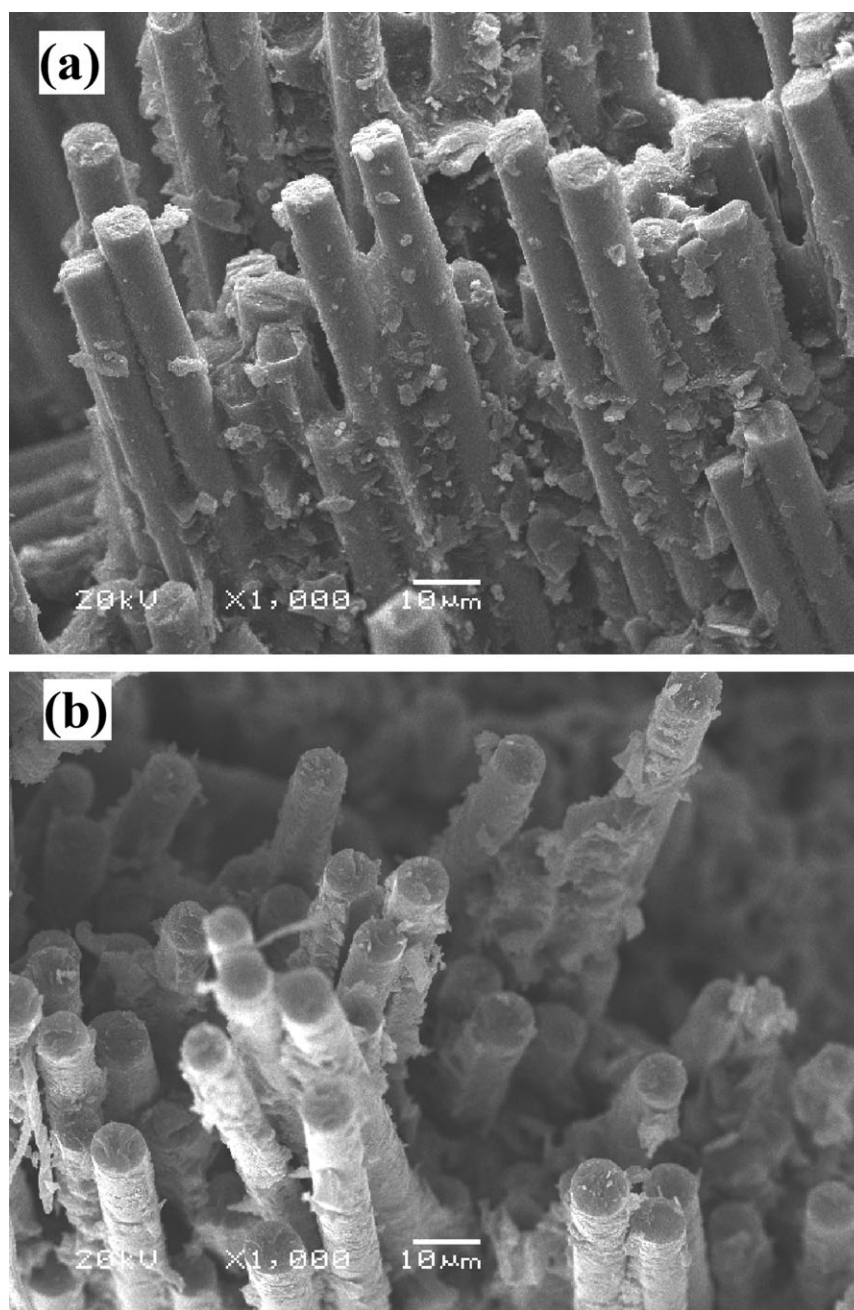


**Figure 10.** SEM images of fracture surfaces of (a) BA-ph/GF composite laminate, (b) EP/BA-ph/GF composite laminates with 40 wt % of EP.

these results revealed that processing temperature could accelerate the copolymerization reaction of EP/BA-ph. From Figure 7, the processing time and polymerization rate of EP/BA-ph systems could be easily controlled by varying the processing temperature and the optical processing temperature for EP/BA-ph copolymers was about 200°C.

Thus, 200°C was chosen to investigate the effect of EP content on the processability of EP/BA-ph copolymers, as shown in Figure 8. It can be seen that pure BA-ph exhibited relatively high initial  $\eta^*$  and the  $\eta^*$  gradually increased until long-playing curing reaction occurred. The initial  $\eta^*$  of EP/BA-ph copolymers, however, decreased with the increasing EP content. Generally,

the low initial  $\eta^*$  can offer convinces for processing such as fully mixing and removal of air bubbles, which is beneficial to practical operations and the final properties of products. Figure 8 also shows that with more EP content, the time for cure reaction of EP/BA-ph copolymers became less, indicating that the EP can accelerate the polymerization reaction rate of BA-ph. This is due to the fact that ring-opening of EP at low temperature can catalyzed the ring-opening of benzoxazine rings and the ring-formation polymerization of the cyano groups. From these results, it is clear that EP/BA-ph copolymer at processing temperature of 200°C exhibited better processing advantages than pure BA-ph while the processability of EP/BA-ph copolymers could be varied by the content of EP.

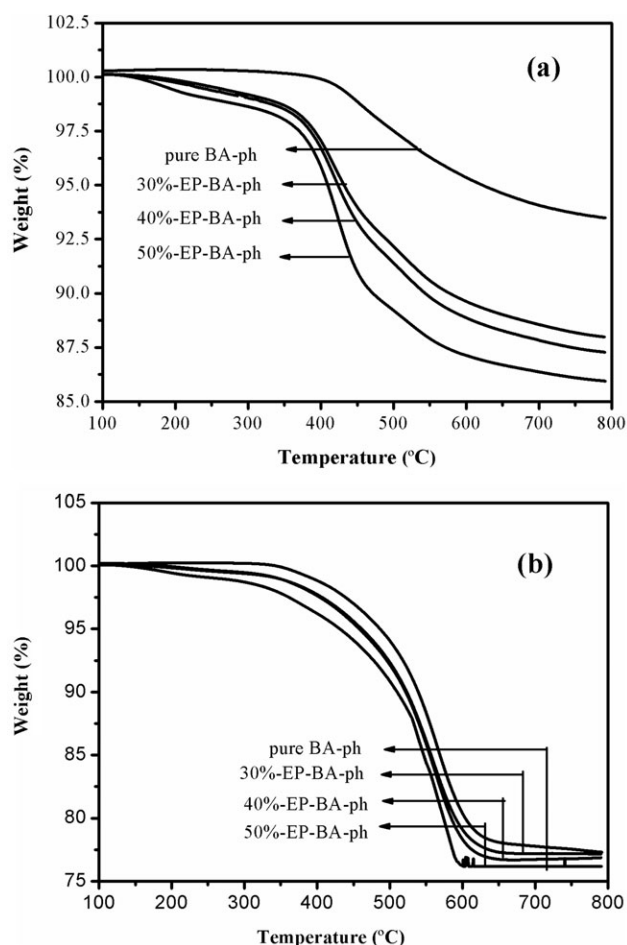


**Figure 11.** TGA curves of EP/BA-ph/GF composite laminates (a) in nitrogen, (b) in air.

### Mechanical Properties of EP/BA-ph/GF Composites

In the previous parts, copolymerizing behavior and processability of EP/BA-ph copolymers were investigated. These investigations can provide us effective mold procedures to prepare GF-based EP/BA-ph composite laminates. Thus, twenty layers of GF prepreg cloth was placed in a stainless steel mold and hot-pressed for the preparation of EP/BA-ph/GF composites under a pressure of 20 MPa at 200°C for 2 h, 230°C for 3 h, 260°C for 3 h, and 280°C for 3 h, respectively and the mechanical properties of resulted EP/BA-ph/GF composite laminates with various EP content was shown in Figure 9. Overall, the trend is

that the flexural properties of the EP/BA-ph/GF laminates were dramatically increased with the increase of EP content. The flexural strength and flexural modulus of BA-ph/GF composites was 511 MPa and 25 GPa, respectively. EP/BA-ph/GF composites with 50 wt % EP content exhibited high flexural strength of 580 MPa and high flexural modulus of 31 GPa, increased by 13.5 and 20% in comparison with those of only BA-ph/GF composites, respectively. In comparison with those of only EP/GF composite laminates, the EP/BA-ph/GF composite laminates did exhibit much better mechanical properties. For example, Yang et al.<sup>32</sup> have prepared EP/GF composite laminates with three kinds of GFs: plain weave fabric GF and biaxial or uniaxial stitched plain weave fabrics GF; and the corresponding flexural strengths of resulted EP/GF composite laminates are 370, 233, and 326 MPa, respectively. Mouritz et al.<sup>33</sup> also reported that EP/GF composite laminates exhibited a relatively low mechanical performance with the flexural strength of 212 MPa and flexural modulus of 12.9 GPa. Compared with those of binary EP/GF composite laminate systems, however, much better mechanical properties were reported in the three-component EP/GF/polymer or EP/GF/filler composite laminate systems. For example, Hameed et al.<sup>34</sup> reported the EP/SAN/GF composite laminates showed a flexural modulus as high as 15 GPa. Lin et al.<sup>35</sup> prepared clay-filled EP/GF composite laminates with the flexural strength of 1000 MPa and flexural modulus of 15 GPa.

Generally, mechanical properties polymer/GF composite laminates depend on the properties of each primary component, the nature of the interface, and the locus of filler-matrix interaction between the matrix resins and GFs.<sup>36</sup> In these EP/BA-ph/GF systems, the dramatic mechanical increments of EP/BA-ph/GF composites could be attributed to multiple factors. These mechanical enhancements, on the one hand, can be attributed to primary component of GF and matrices themselves, since that GF is well known for its high specific strength and stiffness both in tension and in compression while EP and especially BA-ph are also traded for their well mechanical performances. On the other hand, such mechanical enhancements can be due to improvement of interfacial adhesions by the copolymerizing of EP/BA-ph blends. In addition, the excellent wetting properties of EP and polar groups such as phenolic hydroxyl groups generated by the ring-opening of BA-ph and EP may further promote interfacial adhesions, which were confirmed by the SEM images of fracture surfaces of the EP/BA-ph/GF composites, as shown in Figure 10.

As can be seen from Figure 10(a), the fracture surfaces of pure BA-ph/GF composites had little remnant of benzoxazine,

**Table I.** Thermal and Thermo-Oxidative Stabilities of EP/BA-ph/GF Composite Laminates

Samples	N <sub>2</sub>			Air		
	T <sub>i</sub> (°C)	T <sub>5%</sub> (°C)	T <sub>10%</sub> (°C)	T <sub>i</sub> (°C)	T <sub>5%</sub> (°C)	T <sub>10%</sub> (°C)
0%	454.6	586.3	- <sup>a</sup>	567.1	486.6	539.2
30%	420.7	431.8	577.0	563.9	461.3	523.4
40%	419.6	423.5	543.6	562.8	458.2	521.8
50%	418.4	409.4	471.6	554.6	431.5	510.1

<sup>a</sup>Weight loss can not reach 10% at 800°C.



showing a lot of grooving and crevices of bare GFs. In addition, the benzoxazine on the GF surfaces tends to aggregate to form uneven large particles. These results implied that benzoxazine had poor wetting properties with GF, and the fracture occurred between the matrix resins and GF because of the poor interfacial adhesion strength. On the contrary, the fracture surface of EP/BA-ph/GF composites was homogeneously covered by the benzoxazine and EP. This is because that the decrease of  $\eta^*$  in EP/BA-ph copolymers can offer conveniences to make GF be well wetted during the brush-coating process. Moreover, the surface of GF showed wavelike or threadlike patterns, indicating strong interfacial adhesions between GF and matrices. These structures could lead to effective stress transfer and prevent crack initiation and propagation. All these results confirmed the enhancement of mechanical performances.

### Thermal Stabilities of the EP/BA-ph/GF Composites

The thermal decomposition of the EP/BA-ph/GF composites was also examined by TGA (Figure 11) and the main results were summarized in Table I, in which the initial degradation temperature ( $T_i$ ), the temperatures at weight loss of 5% ( $T_{5\%}$ ) and 10% ( $T_{10\%}$ ) were displayed. Overall, thermal and thermo-oxidative stabilities of EP/BA-ph/GF composites in  $N_2$  and air atmosphere were decreased by the increasing EP content, which can be attributed to the relatively low thermal and thermo-oxidative stabilities of EP itself. Nevertheless, all EP/BA-ph/GF composites could stand high temperature up to 470°C in  $N_2$  and 510°C in air, and the characteristic data of thermal and thermal-oxidative stability is shown in Table I. Neat BA-ph/GF composite laminates could stand high temperature above 580°C in  $N_2$  and 530°C in air, respectively. Compared with other state-of-the-art thermosetting composite laminates, the EP/BA-ph/GF composite exhibited excellent thermal and thermal-oxidative stability. The phthalonitrile-based composites or laminates,<sup>25,37–39</sup> by comparison, showed as high  $T_i$  and  $T_{5\%}$  as EP/BA-ph/GF systems. However, these composites have to be cured at elevated temperatures (over 350°C) for a very long time (24 h or even more), which would be hard in the practical processing. The thermosetting polyimide-based composite laminates, on the other hand, are durable for a long time at 343°C, but these laminates showed relatively low mechanical properties (flexural strength: 345 MPa; flexural modulus: 20.7 GPa) compared with EP/BA-ph/GF systems (flexural strength: 580 MPa; flexural modulus: 31 GPa). The other laminates did not maintain the same degree of thermal and oxidative stability<sup>39</sup> as EP/BA-ph/GF systems; meanwhile, the high-temperature machining increased the difficulty of processing and limited their potential applications. To sum up, the excellent thermo-oxidative stabilities and high mechanical properties, together with sound processing conditions could enable the EP/BA-ph/GF composite laminates to find uses under some practical critical circumstances with requirements of high wears and temperatures.

### CONCLUSIONS

Copolymerizing behavior and processability of BA-ph/EP systems were investigated. The results indicated polymerization of BA-ph/EP copolymers was progressing at the ranges from 180 to 200°C. The processing time and polymerization rate of

EP/BA-ph copolymer could be easily controlled by varying the processing temperature and the optimal processing temperature for EP/BA-ph copolymer was about 200°C. EP/BA-ph copolymer exhibited better processing advantages than pure BA-ph while the processability of EP/BA-ph copolymers could be tuned by the content of EP. BA-ph/EP copolymers were used to prepare GF-filled BA-ph/EP composite laminates and their mechanical, morphological and thermal properties were investigated. Compared with those of BA-ph/GF laminates, the flexural strength and flexural modulus of EP/BA-ph/GF composites with 50 wt % EP content were increased by 13.5 and 20%, respectively. Such mechanical enhancements can be due to primary component and the effect of EP on the interfacial interactions. Thermal properties revealed that all EP/BA-ph/GF composites could stand high temperature up to 470°C in  $N_2$  and 510°C in air. These characteristics could enable the EP/BA-ph/GF composites to find uses under some critical circumstances with requirements of excellent mechanical properties and high temperature resistance.

### ACKNOWLEDGMENTS

The authors thank for financial support of this work from the National Natural Science Foundation (No. 51173021) and “863” National Major Program of High Technology (2012AA03A212).

### REFERENCES

- Warrier, A.; Godara, A.; Rochez, O.; Rochez, O.; Mezzo, L.; Luiz, F.; Gorbatiikh, L.; Lomov, V. S.; VanVuure, W. A.; Verpoest, I. *Compos. A Appl. S* **2010**, *41*, 532.
- Jingjing, Q.; Chuck, Z.; Ben, W.; Richard, L. *Nanotechnology* **2007**, *17*, 275708.
- Marsh, G. *Mater. Today* **2003**, *6*, 36.
- Kong, C.; Bang, J.; Sugiyama, Y. *Energy* **2005**, *30*, 2101.
- Brond, S. P.; Lillholt, H.; Lystrup, A. *Annu. Rev. Mater. Res.* **2005**, *35*, 505.
- Moritis, G. H. *Oil Gas J.* **2003**, *101*, 54.
- Weisshaus, H.; Kenig, S.; Siegmann, A. *Carbon* **1991**, *29*, 1203.
- Dillon, F.; Thomas, K. M.; Marsh, H. *Carbon* **1993**, *31*, 1337.
- Agag, T.; Takeichi, T. *Macromolecules* **2001**, *34*, 7257.
- Brunovska, Z.; Lyon, R.; Ishida, H. *Thermochim. Acta* **2000**, *357/358*, 195.
- Allen, D. J.; Ishida, H. *J. Polym. Sci. B Polym. Phys.* **1996**, *34*, 1019.
- Low, H. Y.; Ishida, H. *Macromolecules* **1997**, *30*, 1099.
- Jin, K. H.; Brunovska, Z.; Ishida, H. *Polymer* **1999**, *40*, 1815.
- Goward, R. G.; Sebastiani, D.; Schnell, I.; Spiess, W. H.; Ho-Dong, K.; Ishida, H. *J. Am. Chem. Soc.* **2003**, *125*, 5792.
- Guoping, C.; Wenjin, C.; Xiaobo, L. *Polym. Degrad. Stab.* **2008**, *93*, 739.
- Guoping, C.; Wenjin, C.; Junji, W.; Wenting, L.; Xiaobo, L. *Express. Polym. Lett.* **2007**, *1*, 512.



17. Ning, X.; Ishida, H. *J. Polym. Sci. A Polym. Chem.* **1994**, *32*, 1121.
18. Ishida, H.; Ohba, S. *Polymer* **2005**, *46*, 5585.
19. Sumner, M. J.; Sankarapandian, M.; McGrath, J. E.; Riffle, J. S.; Sorathia, U. *Polymer* **2002**, *43*, 5069.
20. Chaisuwan, T.; Ishida, H. *J. Appl. Polym. Sci.* **2006**, *101*, 548.
21. Pihtili, H. *Eur. Polym. J.* **2009**, *45*, 149.
22. Klein, D. H.; Jorg, K. C. *Surf. Coat. Inter. B Coat. Trans.* **1998**, *81*, 72.
23. Perrin, F. X.; Nguyen, M. H.; Vernet, J. L. *Eur. Polym. J.* **2009**, *45*, 1524.
24. Yuan, M.; Xinghong, Z.; Binyang, D.; Boxuan, Z.; Xin, Z.; Guorong, Q. *Polymer* **2011**, *52*, 391.
25. Keller, T. M. *J. Polym. Sci. A Polym. Chem.* **1988**, *26*, 3199.
26. Fang, Z.; Xiaobo, L. *J. Appl. Polym. Sci.* **2010**, *117*, 1469.
27. Ishida, H.; Rimdusit, S. *Thermochim. Acta.* **1998**, *320*, 177.
28. Ishida, H.; Rodriguez, Y. *Polymer* **1995**, *36*, 3151.
29. Rimdusit, S.; Ishida, H. *Polymer* **2000**, *41*, 7941.
30. Ishida, H.; Rodriguez, Y. *J. Appl. Polym. Sci.* **1995**, *58*, 1751.
31. Rimdusit, S.; Ishida, H. *Rheol. Acta.* **2002**, *41*, 1.
32. Yang, B.; Kozey, V.; Adanur, S.; Kumara, S. *Compos. B* **2000**, *31*, 715.
33. Mouritza, A. P.; Mathys, Z.; Gardiner, C. P. *Compos. B* **2004**, *35*, 467.
34. Hameed, N.; Sreekumar, P. A.; Francis, B.; Yang, W. M.; Thomas, S. *Compos. A* **2007**, *38*, 2422.
35. Li, Y. L.; Lee, J. H.; Hong, C. E.; Yoo, G. H.; Advani, S. G. *Compos. Sci. Technol.* **2006**, *66*, 2116.
36. Prashantha, K.; Soulestin, J.; Lacrampe, M. F.; Claes, M.; Dupin, G.; Krawczak, P. *Express. Polym. Lett.* **2008**, *10*, 735.
37. Warzel, M. L.; Keller, T. M. *Polymer* **1993**, *34*, 6153.
38. Sastri, S. B.; Armistead, J. P.; Keller, T. M. *Polym. Compos.* **1996**, *17*, 816.
39. Kuznetsov, A. A.; Semenova, G. K. *Russ. J. Gen. Chem.* **2010**, *80*, 2170.